

# Multi-walled Carbon Nanotube Film Sensor for Ethanol Gas Detection

Dongzhi Zhang\*, Kai Wang, Jun Tong, Bokai Xia

College of Information and Control Engineering, China University of Petroleum (East China), Qingdao, 266580, China

\*Corresponding author. e-mail: dzzhang@upc.edu.cn

## Abstract

A kind of resistance-type multi-wall carbon nanotubes (MWNTs) film sensor was fabricated using layer-by-layer self-assembly, and an astable multivibrator circuit was designed for resistance measurement. The electrical properties of MWNTs film sensor were investigated, and also its ethanol gas-sensing properties with varying gas concentration are characterized at room temperature. The experiment results shown that the layer-by-layer self-assembled MWNTs film sensor have swift response and high sensitive resistance change when exposed to ethanol gas. This sensor architecture feature advantages such as small-size, low expense, and enjoys extensive applications.

**Keywords:** carbon nanotube, layer-by-layer self-assemble, gas sensor, multivibrator circuit

Copyright © 2013 Universitas Ahmad Dahlan. All rights reserved.

## 1. Introduction

Gas detection plays a very important role in the various fields of atmospheric pollution monitoring, toxic gas or volatility poisonous chemical leak, power transformer diagnosis, human health diagnosis [1-2]. Gas sensors based on nanomaterials are also emerging in a large way as the recent trend indicates the preference towards potential applications. Carbon nanotubes (CNTs) have raised expectations as novel sensing materials since their discovery by Iijima in 1991, due to its large surface area to volume ratio, nanoscale structure and hollow center, while carbon nanotube-based gas sensors shows outstanding features such as fast response, high sensitivity, and operating at room temperature [3-9]. Carbon nanotubes-based thin film can convert the information in relation with gas type and concentration into electrical signals when exposed to different gases, such as nitrogen dioxide, ammonia, and humidity sensor has also been investigated [10-15].

Currently, the detection and sensing of ethanol gas is important for a variety of purposes including ethanol production, industrial chemical processing, fuel processing and use, societal applications, and physiological research on alcoholism. A large number of commercial ethanol measurement systems are available for several of these applications, but in general, these systems are operated at relatively high power levels and high-temperature, are expensive and bulky, and possess functionality that is more limited than required for a number of applications. Therefore, the use of CNTs-based devices for detection of ethanol vapor has received some attention for sensing in a smaller-size, inexpensive and portable way. L. Yi Sin et al fabricated the Si-substrate sensors using an AC electrophoretic technique so as to form bundled CNTs sensing elements, and proved the feasibility of turning the CNTs sensors into a commercialized alcohol sensor with ultra-low power requirements [16]. Brahim et al fabricated ethanol sensors by drop-casting dilute dispersions of a metal-CNT hybrid material onto quartz substrate electrodes at room temperature, and exhibited significantly improved response to ethanol vapor over a wide concentration range compared to the pure CNT sensor [17]. Liang et al fabricated gas sensors from multiwalled carbon nanotubes (MWNTs) coated with a thin tin oxide layer, which shows good response when dispersed in ethanol gas [18]. SnO<sub>2</sub>/MWNTs have been studied as gas sensing materials, and they exhibit improved ethanol sensing properties such as higher sensitivity and quicker response/recovery at 300 °C [19]. However, the above methods mentioned have some weaknesses, for instance, some of them needs high

temperature to work, while some fabrication processes are complicated and depend on some special instruments.

An alternative cost-effective approach, a solution-based bottom-up assembly process called layer-by-layer (LbL) self-assembly, allowed for sequential adsorption of nanometer-thick monolayers of oppositely charged polyelectrolytes and carbon nanotubes to form a homogeneous hierarchical membrane with a molecular-level control over the architecture. Here we fabricated a MWNTs film-based sensor on the substrate of printed circuit board (PCB) with interdigital electrodes (IDE) using LbL self-assembly, and the electrical properties of MWNTs film sensor involving in IDE finger gap and self-assembled layers are investigated, and also its ethanol gas-sensing properties are characterized. The testing results of the LbL self-assembled MWNTs film sensor indicated a prospective application for ethanol gas detection with high performance and low expense.

## 2. Experiment

### 2.1. Materials

MWNTs were chemically treated with the concentrated acid (3:1 for 98 wt%  $\text{H}_2\text{SO}_4$  : 70 wt%  $\text{HNO}_3$ ), and dispersed in deionized (DI) water with concentration of 2 wt.%. The functionalized MWNTs were negatively charged by carboxylic groups, facilitating the uniformly dispersion of MWNTs into DI water.

Polyelectrolytes used for LbL assembly were 1.5 wt% poly(diallylimethylammonium chloride) [PDDA (Sigma-Aldrich Inc.), molecular weight (MW) of 200K-350K, polycation] and 0.3 wt% poly(sodium 4-styrenesulfonate) [PSS (Sigma-Aldrich Inc.), MW of 70K, polyanion] with 0.5 M NaCl in both for enhancing the ionic strength and polyions adsorption.

### 2.2. Fabrication of Self-Assembled MWNTs Film Sensors

Interdigital electrodes are printed on printed circuit board with an outline dimension of  $1 \times 1$  cm, the interdigital electrodes (IDE) finger gap used are  $200 \mu\text{m}$ ,  $300 \mu\text{m}$ ,  $400 \mu\text{m}$  and  $500 \mu\text{m}$ , the electrode material is Ni/Cu. The Electrode device structure for the sensor is depicted in Figure 1. Here we used LbL self-assembly method to fabricate MWNT thin films, which is illustrated as Figure 2. First, immerse the preprocessed IDE device into solution PDDA for 10 min, then rinse it with DI water and dry with nitrogen flow, followed by immersion in solution PSS for 10 min, then rinse and dry. Repeat once again to form two precursor layers of PDDA/PSS on the substrate for charge enhancement. Afterwards, alternately immerse the IDE substrate into solutions PDDA and MWNTs for  $n$  cycles, the immersion time here used is 10 min for PDDA and 15 min for MWNTs, and intermediate rinsing with DI water and drying with nitrogen flow are required after each monolayer assembly to reinforce the interconnection between layers. Finally the multilayer films  $(\text{PDDA/PSS})_2(\text{PDDA/MWNTs})_n$  are formed, where  $n$  is 1, 3, 5, 7, 9, 11 here, and heat the self-assembled MWNTs film devices under  $80^\circ\text{C}$  for 2 hours as the last step.

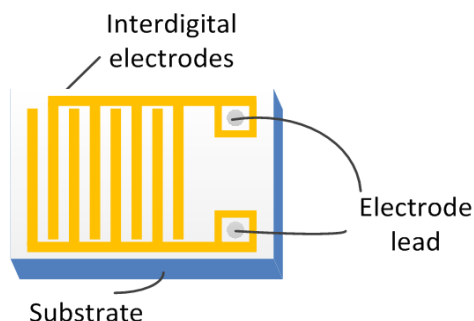


Figure 1. Electrode device structure on a PCB substrate

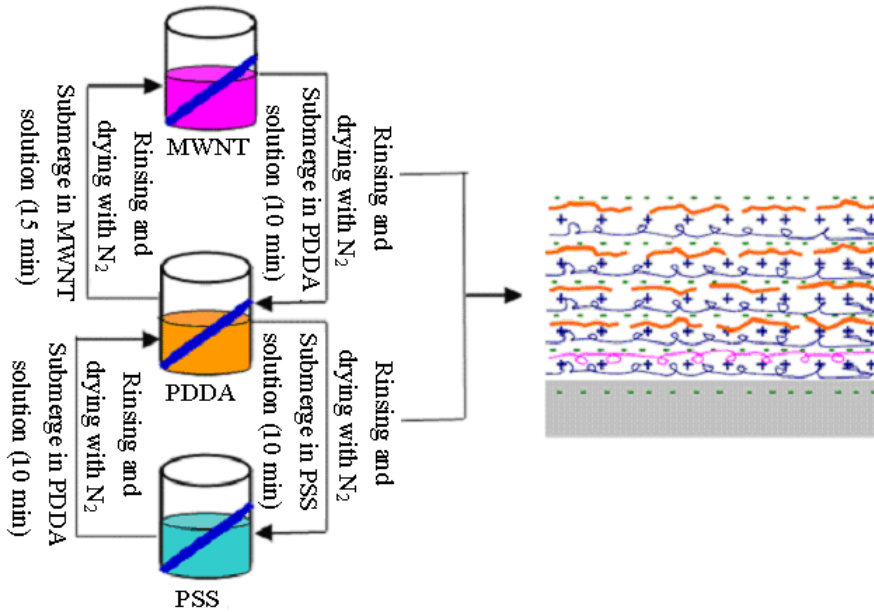


Figure 2. Outline of layer-by-layer self-assembly process

**2.3. Multivibrator Circuit for MWNTs Film Sensors**

A 555 timer operated in astable multivibrator mode was designed for acquiring the resistance signal of MWNT film sensor. The detecting circuit centered around 555 multivibrator is depicted in Figure 3, and the sensor located in the inset of the dotted box. The capacitor is charged and the terminal  $u_o$  has a high level output when the voltage of terminal 2 and 6 less than  $V_{CC}/3$ . And when the voltage of terminal 2 and 6 reaches to  $2V_{CC}/3$ , the capacitor is discharged and the terminal  $u_o$  has a low level output. The working principle for the multivibrator circuit is shown in Figure 4. In such a way, a square wave signal consists of alternate high and low levels is generated from the output terminal  $u_o$ , which is connected to a single microchip or computer for data acquisition.

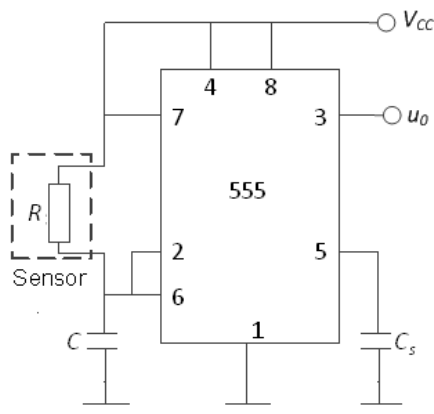


Figure 3. Multivibrator circuit for MWNTs film sensor

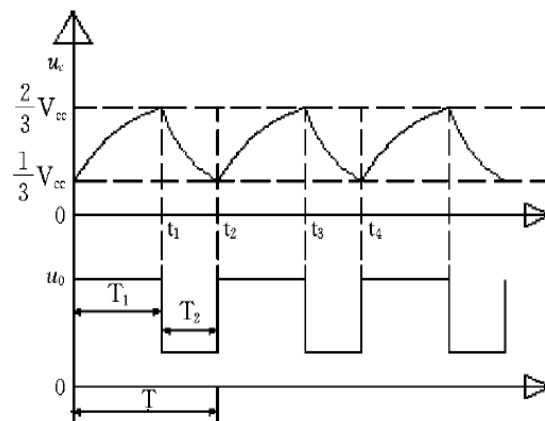


Figure 4. Working principle for the multivibrator circuit

The charge time  $T_1$  and discharge time  $T_2$  for the capacitance are given by

$$T_1 = RC \ln \frac{V_{CC} - V_{CC}/3}{V_{CC} - 2V_{CC}/3} = 0.7RC \quad (1)$$

$$T_2 = RC \ln \frac{V_{CC} - 2V_{CC}/3}{V_{CC} - V_{CC}/3} = 0.7RC \quad (2)$$

The frequency of the astable circuit or multivibrator:

$$f = \frac{1}{T_1 + T_2} = \frac{1}{1.4RC} \quad (3)$$

So the resistance of the MWNTs film sensor is an inverse proportional function of frequency  $f$ , which is given by  $R=1/(1.4Cf)$ . The sensor resistance measurement is achieved by the simple and clearly structured circuit based on multivibrator, signifying low expense and general application.

### 3. Results and Analysis

#### 3.1. Electrical Characterization of the Self-Assembled MWNT Film Sensors

The electrical properties of the fabricated MWNT film devices with different layer numbers are investigated. Figure 5 plots the film resistance for devices with different IDE finger gap and self-assembled layer number, and indicates that the film resistance decreases with the increasing of the assembled layers under the same IDE finger gap, and also shows that it decreases with the increasing of the IDE finger gap under the same layer numbers. The curves in Figure 6 are fitted using the model  $f(x)=a/x^2+b/x+c$ , where  $a$ ,  $b$ ,  $c$  are the undetermined coefficients,  $x$  represents the cycle numbers of self-assembled (PDDA/MWNTs) bi-layers. Table 1 indicates the calculated results for model fitting parameters. Coefficient of determination  $R^2$  is used here as a measure of how well the model fits the experiment data, which is determined as:

$$R^2 = 1 - \frac{\sum_{i=1}^m (y_i - \hat{y}_i)^2}{\sum_{i=1}^m (y_i - \frac{1}{m} \sum_{i=1}^m y_i)^2} \quad (4)$$

where  $y_i$  and  $\hat{y}_i$  represent experimental measured values and predictive values of model, respectively, and  $m$  represents number of measuring points.  $R^2$ , listed in the Table 1, shows the selected models for data fitting are appropriate, and so disclosed the relationships of the film resistance versus assembled layer number and IDE finger gap.

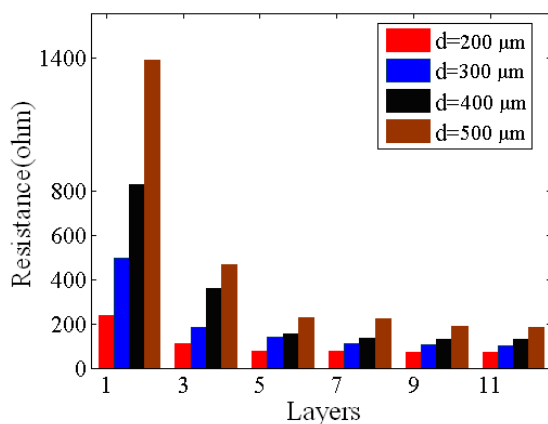


Figure 5. Resistance measurement for LbL thin film with different assembled layers

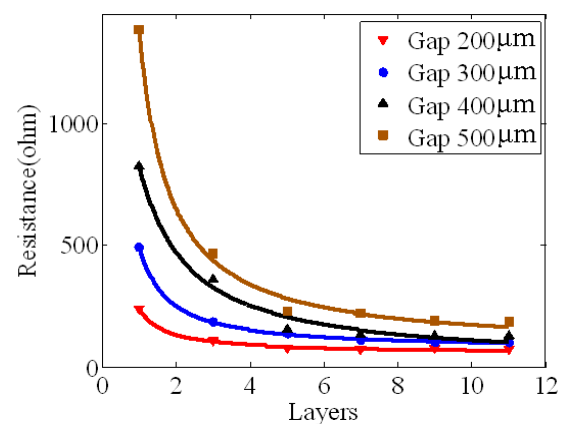


Figure 6. Relations between film resistance and self-assembled layers with different finger gaps

Table 1. Results for model fitting with different IDE finger gaps

Finger Gap $d$ ( $\mu\text{m}$ )	$R^2$	undetermined coefficients		
		$a$	$b$	$c$
500	0.9963	316.2	1002	69.53
400	0.9877	-213.5	1031	9.05
300	0.9994	122.1	302.8	69.12
200	0.9963	59.65	121.4	57.16

### 3.2. Characterization of Ethanol Gas-Sensing Properties

The ethanol gas-sensing experiments are carried out at room temperature. Inject ethanol solution into the sealed beakerflask using a micropipettor and evaporates it completely through heating. Expose the self-assembled MWNTs film sensor (IDE finger gap  $d=200\mu\text{m}$  and layer number  $n=5$ ) into ethanol gas, the adsorption of ethanol gas produced a measurable change in the MWNTs film resistance. The resistance responses to varying ethanol-gas concentration are recorded.

Figure 7 shows the ethanol gas sensing response of the MWNTs film sensor in terms of sensitivity change with changing the concentration of ethanol gas. The sensitivity  $S$  (percentage change in resistance), is denoted as the ratio  $\Delta R/R_{air}$ , where  $\Delta R$  is the difference of resistance of self-assembled MWNTs sensor in the presence of the ethanol gas and in dry air,  $R_{air}$  is the resistance of the sensor in dry air. The results in Figure 7 illustrates that the sensitivity of the MWNTs film sensor increases along with the increasing of gas concentration, and reaches beyond 4% when exposing to ethanol gas concentration of 30 kppm.

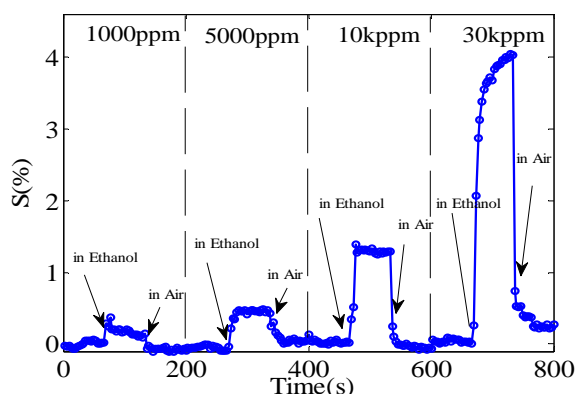


Figure 7. Sensitivity of LbL assembled MWNTs film sensor with varying ethanol-gas concentration

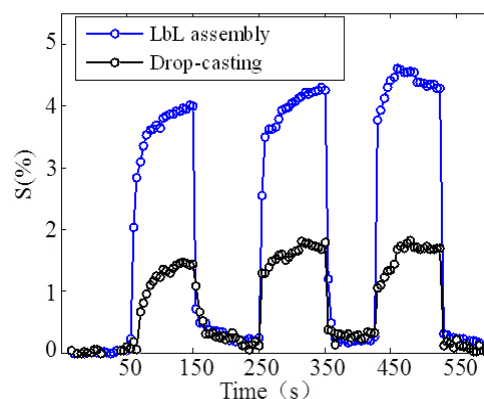


Figure 8. Response to 30 kppm ethanol gas for LbL assembly and drop-casting method

Another alternative method, drop-casting method is used to fabricate MWNTs sensors for making a comparison with LbL self-assembly method. In drop-casting method, the same MWNTs solution and PCB-IDE substrate are employed, and the MWNTs solution is dropped on the substrate surface and then place it under  $80^\circ\text{C}$  for more than 2 hours for drying and forming a MWNT layer. Figure 9 shows the comparative results in response for the two methods when alternating expose to ethanol gas concentration of 30kppm and dry air for three cycles. From the curves in Figure 9 we find that the sensitivity response of LbL self-assembly method is more than two times bigger than that of drop-casting method. The response time of LbL self-assembly method is about 10s and the sensitivity reaches 4.1%, while those of drop-casting method is around 15s and 1.98%, and both the recovery time is about 30s. The LbL self-assembled sensor architecture features advantages such as smaller-size, inexpensive and swift response, and enjoys extensive applications.

It is indicative that the MWNTs film sensor achieves the conversion of the information in relation with ethanol gas concentration into electrical signals. There is an increase of surface potential and subsequent blocking of the movement of conduction electrons when ethanol gas

molecules attached on the surface of MWNTs film, where carboxyl functional groups act as adsorption activation center. The gas sensor presents an increase of resistance in the ethanol gas, one probable reason is that dipole-dipole interactions between the -COOH groups on MWNTs and ethanol molecules leading electrons transfer between the surface and the internal, appearing as resistance increasing. Another reason perhaps is that the adsorption of ethanol molecules directly causes the swelling of the polymer and the increase of tunneling barriers between MWNTs, resulting in an increase of the film resistance.

#### 4. Conclusion

We fabricated MWNT film devices on the substrate of PCB-IDE using LbL self-assembly as gas sensors, and a stable multivibrator circuit was designed for resistance measurement. The electrical properties of MWNTs film devices were investigated through establishing a model involved with number of self-assembled layers and IDE finger gap, and also its ethanol gas-sensing properties are characterized at room temperature. As shown by the experimental results, the LbL self-assembled MWNTs film sensor have a swift response and sensitive resistance change when exposed to ethanol gas, indicated a general application for ethanol gas detection with high-performance and low-cost.

#### Acknowledgements

This work was supported by the Promotive Research Foundation for the Excellent Middle-Aged and Youth Scientists of Shandong Province of China (No. BS2012DX044), the Fundamental Research Funds for the Central Universities of China (No. 12CX04065A), and the Graduate Innovation Engineering Funded Project of China University of Petroleum (No. 12CX-1247).

#### References

- [1] Budi G, Muhammad R, Hendro J. Characterization of Polymeric Chemiresistors for Gas Sensor. *Telkomnika*. 2012; 10(2): 275-280.
- [2] Osama Elsayed G, Mohamed Dessoky A, Ali-Hassan. Comparison between Oil Immersed and SF6 Gas: Power Transformers Ratings. *Telkomnika*. 2012; 10(1): 43-54.
- [3] Iijima S. Helical Microtubules of Graphitic Carbon. *Nature*. 1991; 354(7): 56-58.
- [4] Teerapanich P, MTZ Myint, Joseph CM, Hornyak GL, Dutta J. Development and improvement of carbon nanotube-based ammonia gas sensors using ink-jet printed interdigitated electrodes. *IEEE Transactions on Nanotechnology*. 2013; 12(2): 255-262.
- [5] De Volder MFL, Tawfick SH, Baughman RH, Hart AJ. Carbon nanotubes: present and future commercial applications. *Science*. 2013; 339(6119): 535-539.
- [6] Chuang PK, Wang LC, Kuo CT. Development of a high performance integrated sensor chip with a multi-walled carbon nanotube assisted sensing array. *Thin Solid Films*. 2013; 529: 205-208.
- [7] Hoa ND, Van Quy N, Cho Y, Kim D. Porous single-wall carbon nanotube films formed by in situ arc-discharge deposition for gas sensors application. *Sensors and Actuators B: Chemical*. 2009; 135(2): 656-663.
- [8] Dorval N, Lauret JS, Attal-Trétout B, Loiseau A. Gas sensors based on thick films of semi-conducting single walled carbon nanotubes. *Carbon*. 2011; 49(11): 3544-3552.
- [9] Wang Y, Yeow JTW. A Review of Carbon Nanotubes-based Gas Sensors. *Journal of Sensors*. 2009; 2009: 1-24.
- [10] Xu K, Wu CD, Tian XJ, Liu J, Li MX, Zhang Y, Dong ZL. Single-Walled Carbon Nanotube-based Gas Sensors for NO<sub>2</sub> Detection. *Integrated Ferroelectrics*. 2012; 135: 132-137.
- [11] Peng N, Zhang Q, Chow CL, Tan OK, Marzari N. Sensing Mechanisms for Carbon Nanotube based NH<sub>3</sub> Gas Detection. *Nano Letters*. 2009; 9(4): 1626-1630.
- [12] Faizah MY. Room Temperature Multi Gas Detection using Carbon Nanotubes. *European Journal of Scientific Research*. 2009; 35(1): 142-149.
- [13] Karimov KHS, Ahmed MM, Kariyeva ZM, Saleem M, Mateen A, Moiz SA. Humidity Sensing Properties of Carbon Nanotube Thin Films. *Sensor Letters*. 2011; 9(5): 1649-1653.
- [14] Du N, Zhang H, Chen BD, Ma XY, Liu ZH, Wu JB, Yang DR. Porous Indium Oxide Nanotubes: Layer-by-Layer Assembly on Carbon-Nanotube Templates and Application for Room-Temperature NH<sub>3</sub> Gas Sensors. *Advanced Materials*. 2007; 19(12): 1641-1645.
- [15] Yu HH, Cao T, Zhou LD, Gu E, Yu DS, Jiang DS. Layer-by-Layer Assembly and Humidity Sensitive Behavior of Poly (ethyleneimine)/Multiwall Carbon Nanotube Composite Films. *Sensors and Actuators B: Chemical*. 2006; 119(2): 512-515.

- [16] Mandy LYS, Gary CTC, Gary MKW, Wen JL, Philip HWL, Ka WW. Ultralow-Power Alcohol Vapor Sensors using Chemically Functionalized Multiwalled Carbon Nanotubes. *IEEE Transactions on Nanotechnology*. 2007; 6(5): 571-577.
- [17] Brahim S, Colbern S, Gump R, Moser A, Grigorian L. Carbon Nanotube-based Ethanol Sensors. *Nanotechnology*. 2009; 20(23): 235502-235508.
- [18] Liang YX, Chen YJ, Wang TH. Low-Resistance Gas Sensors Fabricated from Multiwalled Carbon Nanotubes Coated with A Thin Tin Oxide Layer. *Applied Physics Letter*. 2004; 85(4): 666-668.
- [19] Chen YJ, Zhu CL, Wang TH. The Enhanced Ethanol Sensing Properties of Multi-Walled Carbon Nanotubes/SnO<sub>2</sub> Core/Shell Nanostructures. *Nanotechnology*. 2006; 17(12): 3012-3017.